Landslide-generated tsunamis runup at the coast of a conical island: New physical model experiments

M. Di Risio,[1] P. De Girolamo,[1] G. Bellotti,[2] A. Panizzo,[3] F. Aristodemo,[4] M. G. Molfetta,[5] and A. F. Petrillo[5]

Received 9 April 2008; revised 22 September 2008; accepted 3 October 2008; published 20 January 2009.

[1] This paper presents new physical model experiments on tsunamis generated by landslides at the coast of a conical island. The experiments have been carried out in a large wave tank; the radius of the island coastline and the falling height of the landslide have been varied during the experimental campaign. The landslide is reproduced by a solid body shaped as a half of an ellipsoid. Tsunami runup is measured using special wave gauges; a detailed analysis of the runup along the coastline is presented, with special attention to the role of each wave in the packet and to the evolution of the envelope of the first group of waves.

Citation: Di Risio, M., P. De Girolamo, G. Bellotti, A. Panizzo, F. Aristodemo, M. G. Molfetta, and A. F. Petrillo (2009), Landslide-generated tsunamis runup at the coast of a conical island: New physical model experiments, *J. Geophys. Res.*, *114*, C01009, doi:10.1029/2008JC004858.

1. Introduction

[2] Landslide occurring at the coast of the sea can trigger tsunami waves that propagate both offshore and along the coastline. The extension of the landslides is typically much smaller than the tsunamigenic source related to large earthquakes; landslide generated waves are therefore expected to be dangerous especially for the coastal regions located close to the area where the landslide takes place. It is then crucial to study the tsunami properties near the generation area, where the mechanisms of wave generation and propagation over varying bottom can be hardly separated.

[3] Many laboratory experiments have been carried out so far in order to gain insight on the properties of the landslide generated waves. Most of these studies [*Wiegel*, 1955; *Heinrich*, 1992; *Watts*, 1997, 1998, 2000; *Grilli and Watts*, 2005; *Fritz et al.*, 2003a, 2003b] have focused on two-dimensional layouts (1 horizontal, 1 vertical direction) and have provided fundamental information on the process. *Panizzo et al.* [2005] have studied waves generated in a three-dimensional layout but they employed a flat bottom: their results can be applied to describe the generation process but not the interaction of the waves with the coast. *Enet et al.* [2003], *Enet and Grilli* [2005, 2007] and *Liu et al.* [2005] have recently presented three-dimensional investigations, reproducing landslides sliding along sloping beaches. For the experiments by Liu et al. the width of the flumes was 4 times the width of the landslides, and for those by Enet and Grilli about 5.4 times.

[4] The alongshore dimension of the facilities used in these studies was therefore such that the waves reflected at the sidewalls (i.e., those parallel to the cross-shore direction), quickly contaminated the wavefield. M. Di Risio et al. (Three-dimensional experiments on landslide generated waves at a sloping coast, submitted to *Coastal Engineering*, 2008, hereinafter referred to as Di Risio et al., submitted manuscript, 2008) have then tried to overcome this problem and have reproduced in the laboratory a beach 25 times longer than the width of the landslide, but the tank was shorter in the offshore direction. During those experiments the properties of the first generated wave could be properly estimated for a distance, along the coast, of about 10 times the width of the landslide. Then the waves reflected at the offshore walls contaminated the records. Some important parameters such as the maximum runup along the coast, which can be induced also by the second and by the following waves, could not be estimated. A detailed analysis of the near field was successfully given on the basis of video records. It is also worth to cite the work by *Lynett and Liu* [2005], which have performed careful numerical computations of the runup induced by landslide generated waves along a straight sloping coast. Their parametric analysis has also guided the design of the laboratory experiments described herein.

[5] In this paper we present a research which partially overcomes the difficulties of that presented by Di Risio et al. (submitted manuscript, 2008) since the laboratory experiments have been carried out in a large wave tank (30.00 m $\times$ 50.00 m in plan), so that the effect of the waves reflected at the sidewalls is negligible for the first waves. We reproduce

[1]Dipartimento di Ingegneria delle Strutture delle Acque e del Terreno, Laboratorio di Idraulica Ambientale e Marittima, University of L'Aquila, Monteluco di Roio, Italy.
[2]Dipartimento di Scienze dell'Ingegneria Civile, University of Roma Tre, Rome, Italy.
[3]Dipartimento di Idraulica, Trasporti e Strade, University of Roma La Sapienza, Rome, Italy.
[4]Dipartimento di Difesa del Suolo, University of Calabria, Cosenza, Italy.
[5]Dipartimento di Ingegneria delle Acque e di Chimica, Laboratorio di Ricerca e Sperimentazione per la Difesa delle Coste, Technical University of Bari, Bari, Italy.

0148-0227/09/2008JC004858

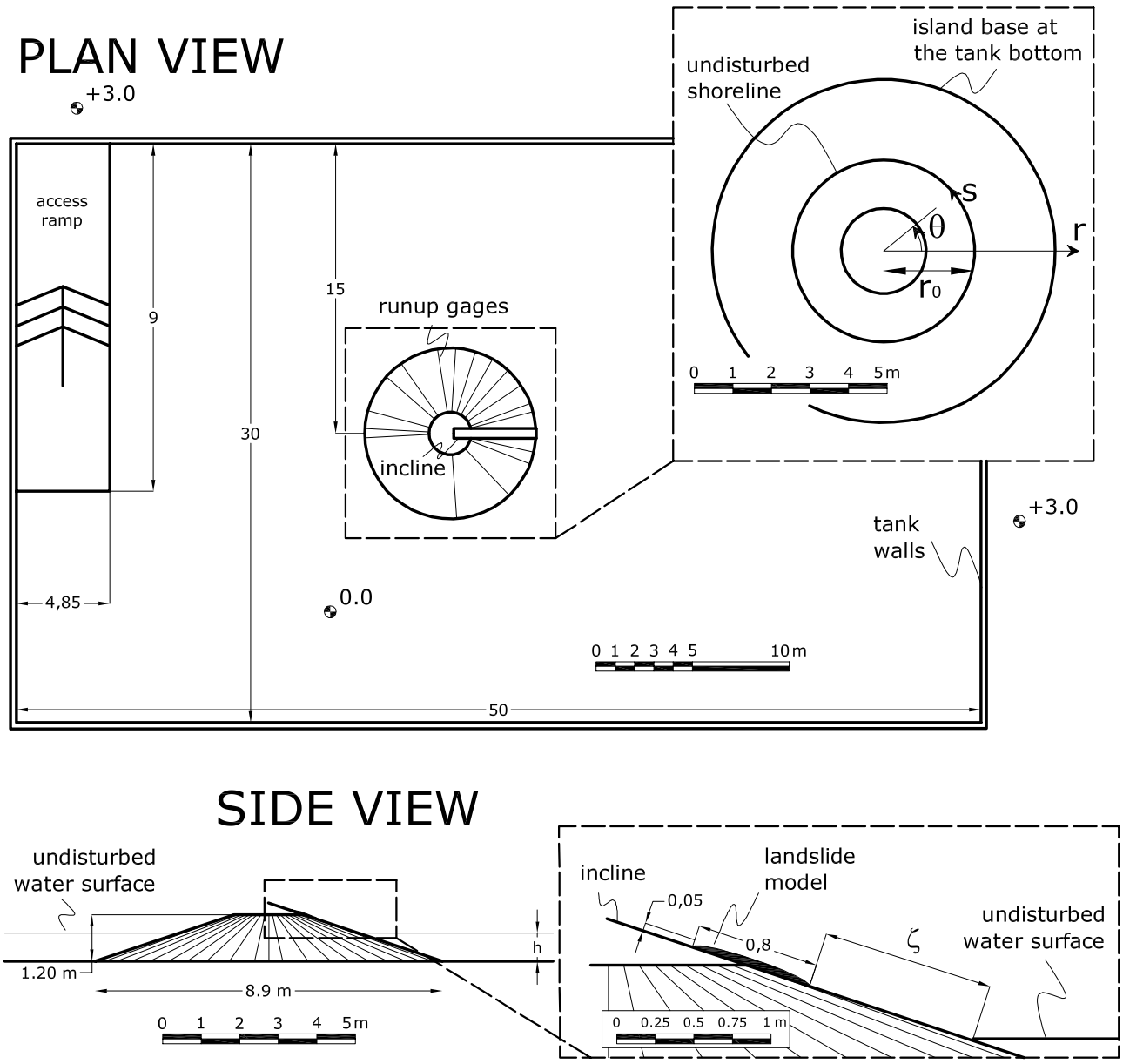

Figure 1. Sketch of the conical island and reference frame (length unit in meters).

a conical island and a landslide sliding along its flank. The geometrical parameters of the island and of the landslide make this experiment suitable to reproduce in a simplified manner and at a small scale (Froude scale, 1:1000) the landslide occurred at the volcanic island of Stromboli (South Tyrrhenian Sea, Italy) on the 30 December 2002 [*Tinti et al.*, 2005a, 2005b]. On that day two large landslides triggered a tsunami that destroyed part of the town of the island.

[6] It is worth to remember that the experiments presented here are similar to those carried out by *Briggs et al.* [1995], but they generated tsunamis that attacked a conical island from offshore, while here, for the first time, the waves are generated along the coast.

[7] The paper is organized as follows. Next section details the physical model layout and the experimental facilities. Results obtained by analyzing the runup of generated waves propagating alongshore are presented in the following section. Discussion and conclusions follow.

2. Layout of the Experiment

[8] The experiments have been carried out in a large wave tank at the Research and Experimentation Laboratory for Coastal Defence (LIC) of the Technical University of Bari (Italy) in cooperation with the Environmental And Maritime Hydraulics Laboratory ''Umberto Messina'' (LIAM) of the University of L'Aquila. The wave tank is 30.00 m wide, 50.00 m long and 3.00 m deep. A truncated conical island (radius at the tank bottom level 4.45 m, height of 1.20 m) has been built at the center of the tank using PVC sheets (thickness 0.01 m) sustained by a steel frame (see Figures 1 and 2). The plastic sheets were stiff enough to prevent any vibration induced by the landslide motion

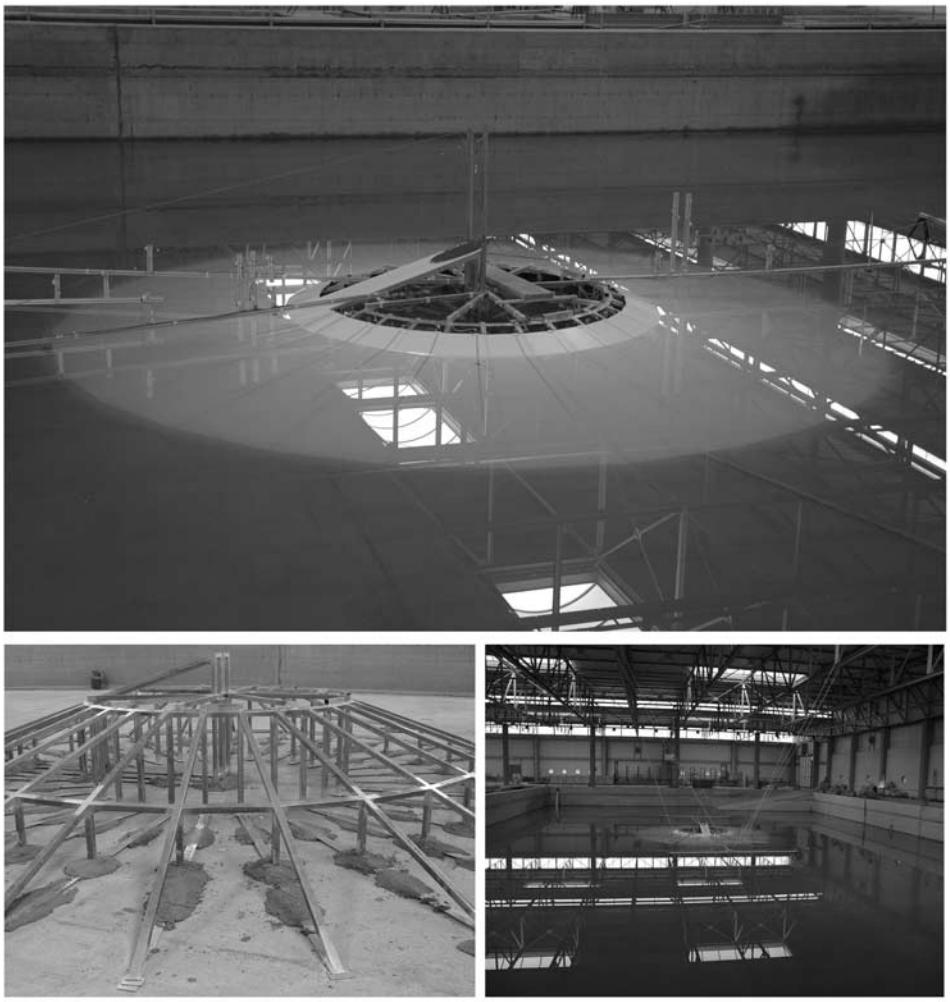

Figure 2. Picture of the (top) conical island during the experiments, (bottom left) the steel frame, and the (bottom right) overall view of the wave tank.

and by the waves. The slope of the flanks of the island is 1/3 (1 vertical, 3 horizontal). By varying the water depth it has been possible to study the waves propagation around islands with different shoreline curvature radius: the radius of the circular shoreline ranged from 2.07 m up to 2.60 m.

[9] The landslide model is identical to that used by Di Risio et al. (submitted manuscript, 2008), it has a regular shape that reproduces a half of an ellipsoid. In a reference frame with the origin placed at the center of the ellipsoid it has the axis a (parallel to the undisturbed shoreline) equal to 0.20 m (landslide width $2a = 0.40$ m), axis b (orthogonal to the undisturbed shoreline) equal to 0.40 m (landslide length $2b = 0.80$ m) and axis c (orthogonal to the flank) equal to 0.05 m (landslide height $c = 0.05$ m) for a total volume $V = 0.0084$ m^3. The density of the landslide is 1.8310^3 kg/m^3 for a total mass of 15.40 kg. The landslide is made up of plastic material covered by an exterior layer of fiberglass and the flat bottom, that is in contact with the flank of the island, is made up of steel. The landslide model was used in the above mentioned experiments by Di Risio et al. (submitted manuscript, 2008), which were carried out reproducing a straight coast. The effect of the curvature of submerged beach now introduces some experimental difficulties since as the landslide model slides down the slope, the curvature of the flank increases. In order to overcome this problem, along the path of the landslide a 0.50 m wide flat slope has been built; it is carefully and smoothly connected to the curved bottom in the surroundings, in order to minimize disturbances on the propagating waves. The resulting geometry is a plane slope connected to the curved flanks of the island. The landslide is constrained to move on rails placed along the slope and therefore it moves exactly along a specified axis. In order to reconstruct the landslide motion a capacitive accelerometer (Metra-Mess CB41) has been placed inside the landslide to measure its acceleration.

[10] The instantaneous displacements of the shoreline have been measured by means of special wave gauges that have been built employing two steel bars (square section of 4 mm $\times$ 4 mm) directly embedded into the PVC of the slope, as in Di Risio et al. (submitted manuscript, 2008). These instruments present higher noise and lower resolution (0.55 mm and 0.50 mm respectively) than the traditional resistive gauges usually employed, but data still remain reliable. All the signals have been acquired simultaneously at a frequency of 1000 Hz; in view of the number of signals to acquire, which were too many for a single D/A acquisi-

Table 1. Angular Positions of Runup Gauges

Gauge Name	Angular Position θ (deg)	Gauge Name	Angular Position θ (deg)
1R	14.5	11R	138.6
2R	20.6	13R	164.6
3R	34.3	14R	176.8
4R	47.6	15R	−176.9
5R	60.2	16R	−85.7
6R	72.9	17R	−46.5
7R	86.3	19R	−20.9
8R	98.7	20R	−12.8
10R	125.2		

tion board, a digital trigger system has been employed to simultaneously collect all the signals of sensors using two computers each one equipped with its own data acquisition board (National Instruments 6024/E and 6052/E). These two PCs have been digitally connected to a switch that sends an electrical signal (5 *V*) to the software used to collect runup gauges time series. When the switch is turned on, the acquisitions start simultaneously on all the PCs.

[11] The reference coordinate system used in the subsequent analysis is presented in Figure 1. The horizontal polar axes r and θ respectively measure the distance from the plan center of the island and the angle, positive counterclockwise, between any line passing from the center of the island and the axis along which the landslide moves. A curvilinear abscissa s is measured counterclockwise along the undisturbed shoreline starting from the point where the landslide enters the water ($r = r_0$, $\theta = 0$); a further variable of interest is the dimensionless curvilinear abscissa defined, consistently with *Lynett and Liu* [2005], as $s' = s/(2a)$, where $2a$ = 0.4 m is the width of the landslide. Table 1 summarizes the positions and the names of the runup gauges.

[12] Three values of the undisturbed shoreline radius r_0 (2.07 m, 2.20 m and 2.60 m) have been used by varying water depth into the tank, in order to study its effect on tsunami induced runup. For each shoreline radius several tests have been performed by varying the height from which the landslide falls into the water which is measured, along the inclined plane, by the distance ζ between the lower point of the landslide and the undisturbed shoreline (see Figure 1). The release distance ζ assumed values of 0.60 m, 0.50 m, 0.40 m and 0.30 m: only subaerial landslides have been studied. The procedure of each test is the same as that described in Di Risio et al. (submitted manuscript, 2008). First the landslide is placed at the selected position along the slope. Then it is waited until the natural oscillations of the water surface in the tank has completely stopped (i.e., several minutes). Then the acquisition process begins, the landslide model is released and the tsunami is generated. Typically, acquisition process stopped when the waves reflected at the sidewalls had completely contaminated the wavefield, that is, about after 30 s. Each test has been repeated twice in order to check for repeatability of the experiments.

3. Landslide Motion

[13] In order to reproduce numerically and analytically the experiments described herein, the correct modeling of the landslide movements is a crucial point. The movements of the landslide have been reconstructed on the basis of the measured acceleration. From a qualitative point of view all the performed tests provided similar results. A sample results, referring to a test carried out using ζ = +0.60 m and undisturbed shoreline radius r_0 equal to 2.07 m, is reported in Figure 3. It shows the landslide acceleration $a(t)$ along with vertical lines that indicate the times at which the landslide hits the water surface and when it becomes totally submerged. The final negative acceleration peak indicates the time at which the landslide suddenly hits the tank bottom, thus stopping. It has to be noted that just after the starting of motion, the acceleration reaches a value near the gravity acceleration acting along the incline direction (equal to 3.1 m/s^2). The acceleration during the underwater phase is almost zero, that is, the buoyancy and the gravitational forces are balanced. Finally, in order to provide suitable data for the reproduction of these experiments using mathematical/numerical models, Figure 4 shows the landslide velocity $v(t)$ (dashed line) and the instantaneous position along the incline $s(t)$ (solid line) that have been computed by integrating the measured accelerations. Figure 4 refers to the tested values of the release distance ζ and for the tests carried out with undisturbed shoreline radius r_0 equal to 2.07 m. It is worth to comment that the velocities variation occurring during the aerial phase (i.e., between 0.25 ÷ 0.60 s) and during the underwater phase (i.e., between 2.00 ÷ 2.25 s) are due to the fact that the landslide slides over the junction of two sheets of PVC; although these have been carefully aligned some small disturbance to the motion could not be avoided.

4. Description of Results

[14] Figure 5 shows the sequence of images collected during one of the experiments. Light effects on water

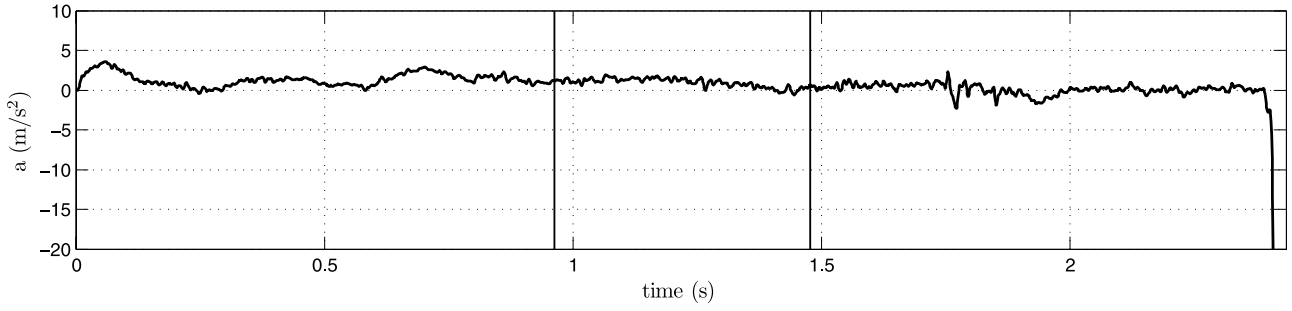

Figure 3. Landslide accelerations measured during the test run with ζ = 0.60 m and undisturbed shoreline radius equal to 2.07 m. Vertical lines refer to time instants when the landslide hits the water surface and when the landslide becomes totally submerged.

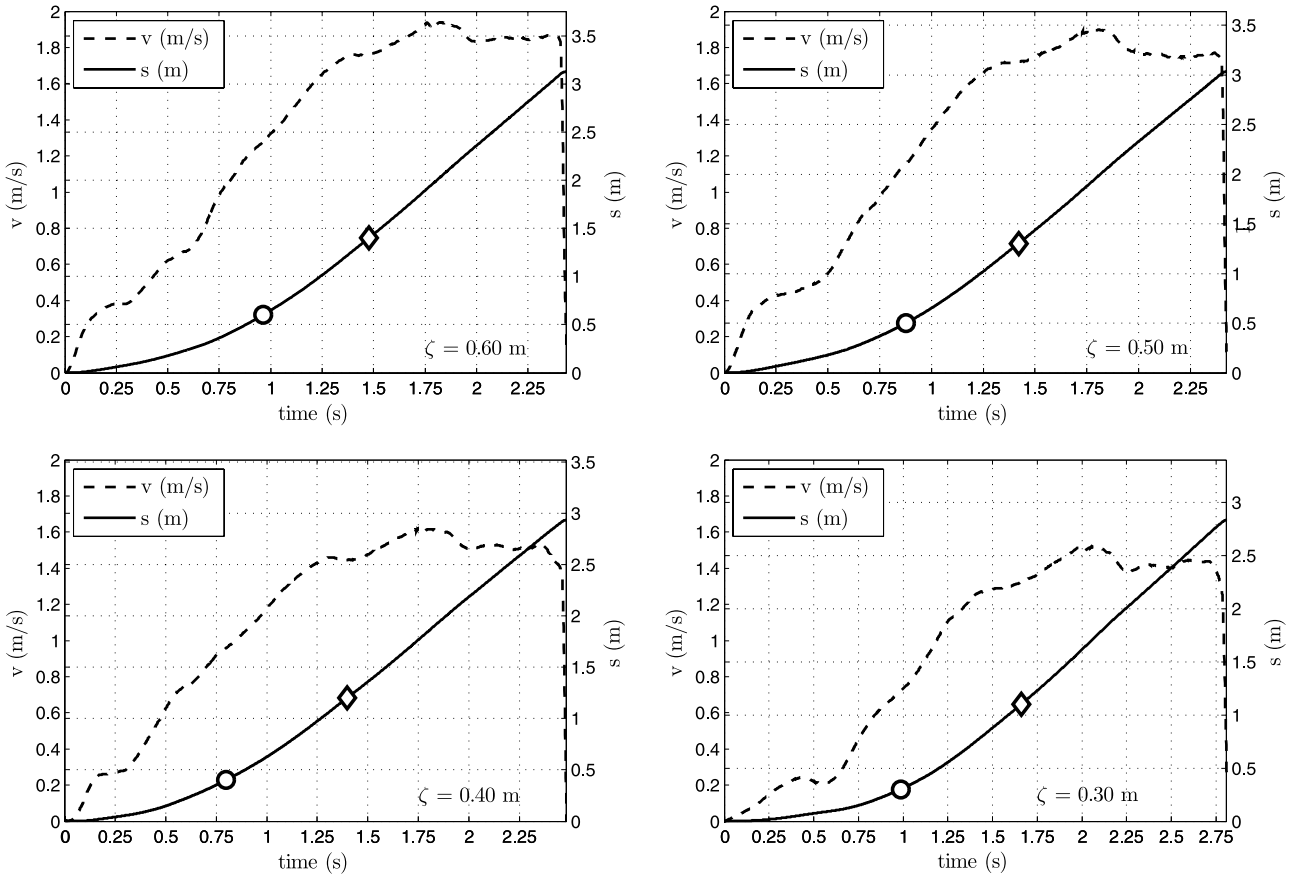

Figure 4. Landslide velocity (dashed lines) and sliding distance (solid lines) for different release distances and undisturbed shoreline radius equal to 2.07 m. Circles refer to time instant when the landslide hits the water surface, and diamonds refer to time instant when the landslide becomes totally submerged.

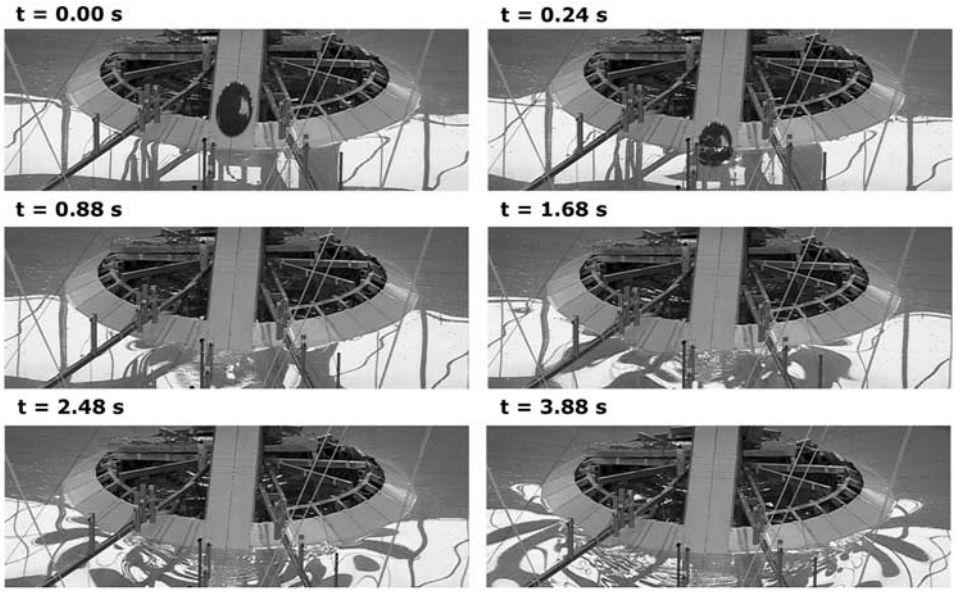

Figure 5. Sequence of images collected during one of the experiments. Light effects allow recognizing of generated waves pattern, especially of waves propagating along the island coastline.

surface allow to recognize the waves and it is possible to see the waves propagating along the shoreline (i.e., t = 3.88 s).

[15] Sample records of the runup gauges for an experiment carried out using $r_0 = 2.07$ m (water depth $h = 0.80$ m) and $\zeta = 0.40$ m (but very similar results have been obtained for different values of this parameter) are presented in Figures 6 and 7. On each subplot the instantaneous vertical elevation of the shoreline position is reported; a small circle and a line are used on each plot to indicate the position of the runup gauges on the island flanks. It is worth to stress that gauges 1R and 20R, 2R and 19R, 4R and 17R, 7R and 16R, 14R and 15R are placed at points which are almost symmetrical about the axis passing through the landslide path in order to check the symmetry of wave propagation along the coast (see Figure 8 for a comparison of elevation time series collected by means of 2R−19R and 7R−16R runup gauges).

[16] The first generated wave always has first a crest followed by a trough. At gauge 1R ($s = 0.52$ m, $s' = 1.3$) the trough is larger (in absolute value) than the crest ($a^+/a^- = 0.64$, being a^+ and a^- the crest and the trough amplitude respectively); the maximum runup and the minimum rundown are given by the first wave, that has a period of 2.4 s (estimated by means of zero-up crossing method). The second wave has a double-peaked crest and a small trough ($a^+/a^- = 2.1$) and its period is of 2.3 s, almost equal to that of the first wave. At gauge 2R ($s = 0.74$ m, $s' = 1.9$) the crest of the first wave (period of 1.6 s) still gives the maximum runup, larger than that obtained at the previous gauge and the trough amplitude still is larger than the crest one ($a^+/a^- = 0.78$). The second wave here has a larger crest than that measured at gauge 1R, while the trough appears to be extremely small ($a^+/a^- = 8.4$); its period increases again up to 2.3 s. At gauge 3R ($s = 1.24$ m, $s' = 3.1$) the crest of the first wave is again smaller than the following trough ($a^+/a^- = 0.59$) with a wave period equal to 1.9 s. The maximum runup is now given by the second wave, which still appears to be double peaked, and its crest is again larger than the trough ($a^+/a^- = 2.3$) with the period remaining almost constant (1.7 s). At gauge 4R ($s = 1.24$ m, $s' = 3.1$) the second wave (period of 1.8 s), also here responsible of the maximum runup, is definitely larger than the first one. At gauges 5R, 6R and 7R the crest of the first wave is much smaller than the following trough (wave period higher than 2.4 s), while the crest of the second wave is high and very sharp with wave period that does not exceed the value of 1.8 s. The records obtained at these gauges also allow identification of waves that are propagating in the opposite direction along the island coast. At gauge 8R the maximum runup is given by the third wave. At gauge 10R it can be seen that the first wave packet is superposing by the counter propagating waves. At gauge 11R it is no longer possible to visually separate the two waves systems. At gauge 13R the two wave packets are superposed and the maximum runup is now given by the fifth wave; at gauge 14R the fourth wave gives the maximum runup.

[17] Results can be also usefully viewed in terms of plan snapshots of the shoreline displacements as shown in Figure 9 for the experiment with $\zeta = 0.40$ m and $r_0 = 2.07$ m. Wave runup measured at the gauges has been plotted for few important times, chosen as those at which the maximum runup is measured at each gauge. More clearly, the maximum runup occurs at $t = 2.7$ s for $\theta = 14.5°$ (gauge 1R), at $t = 3.1$ s for $\theta = 20.6°$ (gauge 2R), and so on. Only half of the island coast has been plotted; the dark arrow represents the point at which the landslide enters the water, the dashed semicircle represents the undisturbed shoreline position and the two solid semicircles give the scale of flooding representing horizontal displacement of shoreline of ±0.01 m. The thick solid line passes through the points of maximum runup at each gauge. This analysis is useful to investigate how the coast of the island undergoes the inundation during the tsunami propagation. and allows to get an idea of the length of the waves. For example at $t = 4.9$ s the crest of the first wave has a length approximately equal to the distance between the gauge 7R and a point near gauge 5R. The total length of the first wave can be roughly estimated as 2.4 m, that is, 6 times the landslide width. Similar values have been obtained for the other waves and for the other experiments.

[18] In the Figure 10a the maximum runup ($R_u^{(\max)}$) and the minimum rundown ($R_d^{(\max)}$) at each gauge are reported. Each value has been plotted using a different symbol depending on which wave induced $R_u^{(\max)}$ and $R_d^{(\max)}$: the first wave is indicated by a small circle, the second by a square, the third by a diamond and the fourth by a triangle. On Figures 10b to 10e the maximum runup and rundown given by the first four waves are presented. These data refer to the tests with undisturbed shoreline radius equal to $r_0 = 2.07$ m. All the results obtained for the two repetitions and by using different values of ζ, for a total of 8 experiments, have been plotted together, in order to check for repeatability and dependence on ζ.

[19] The first important evidence is that the maximum runup and the minimum rundown increase in the near field and then decrease as the distance from the generation area grows. At about $s' = 3$ there is the maximum inundation of the coast. In the area opposite to that where the landslide enters the water ($\theta > 90°$) the inundation increases again because of the superposition with waves propagating in the opposite direction along the coast. The maximum values of $R_u^{(\max)}$ are given by the first wave for the first two gauges (i.e., $s' \leq 2.1$), by the second wave in the region for which $3.2 \leq s' \leq 7.9$ and by the third wave for $9.1 \leq s' \leq 12.5$. The minimum rundown is given by the first wave up to $s' = 5.8$, then in the region $6.6 \leq s' \leq 8.9$ the second trough is the deepest one and for $11.3 \leq s' \leq 12.5$ the third trough induces the minimum rundown.

[20] The runup of the first wave has a maximum at the gauge 2R, then it rapidly decreases. The results obtained for the two repetitions of each test and for the 4 values of ζ appear to be extremely similar. For the runup $R_u^{(1)}$ given by the first crest the results are almost identical; the values of $R_d^{(1)}$ may differ of few percentage points very close to the generation area ($s' \leq 3.25$), while are almost identical elsewhere. This ensures, on the one hand, the repeatability of the results and on the other hand that the first wave properties are weakly influenced by landslide falling height ζ. For the second wave, the results appear to differ one from each other. In particular, we have found that the results of each repetition (i.e., by using the same ζ) present differences of the same order of magnitude of those obtained varying ζ and the values of $R_u^{(2)}$ appear to be more dispersed than the rundown $R_d^{(2)}$. The maximum inundation given by the second wave is at the gauge 3R ($s' = 3.25$). The results

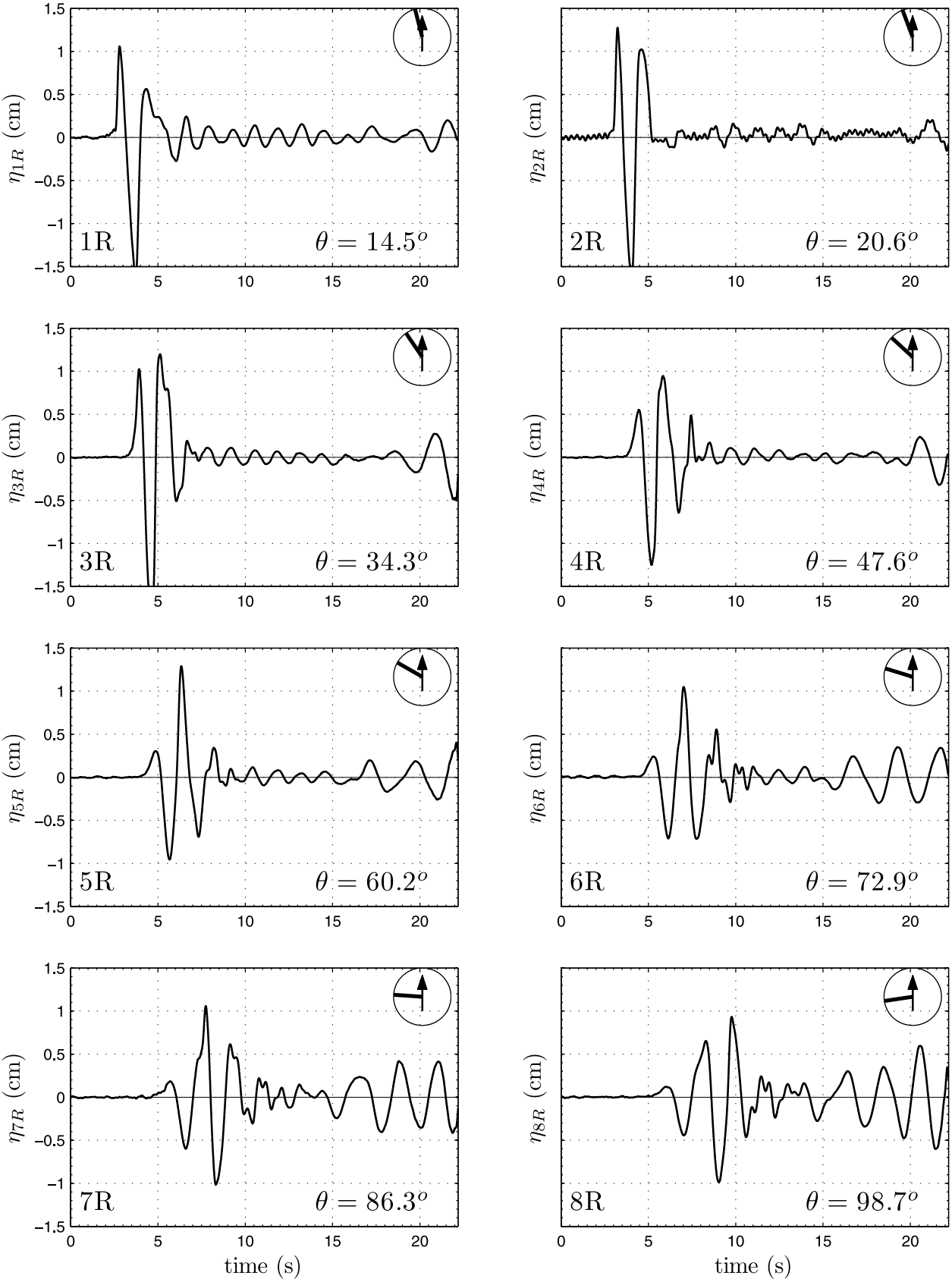

Figure 6. Runup (η) time series measured during experiments with ζ = 0.40 m and r_0 = 2.07 m. The small circle on each plot reproduces the coastline, the arrow indicates where the landslide enters the water, and the line specifies the position of the considered runup gauge.

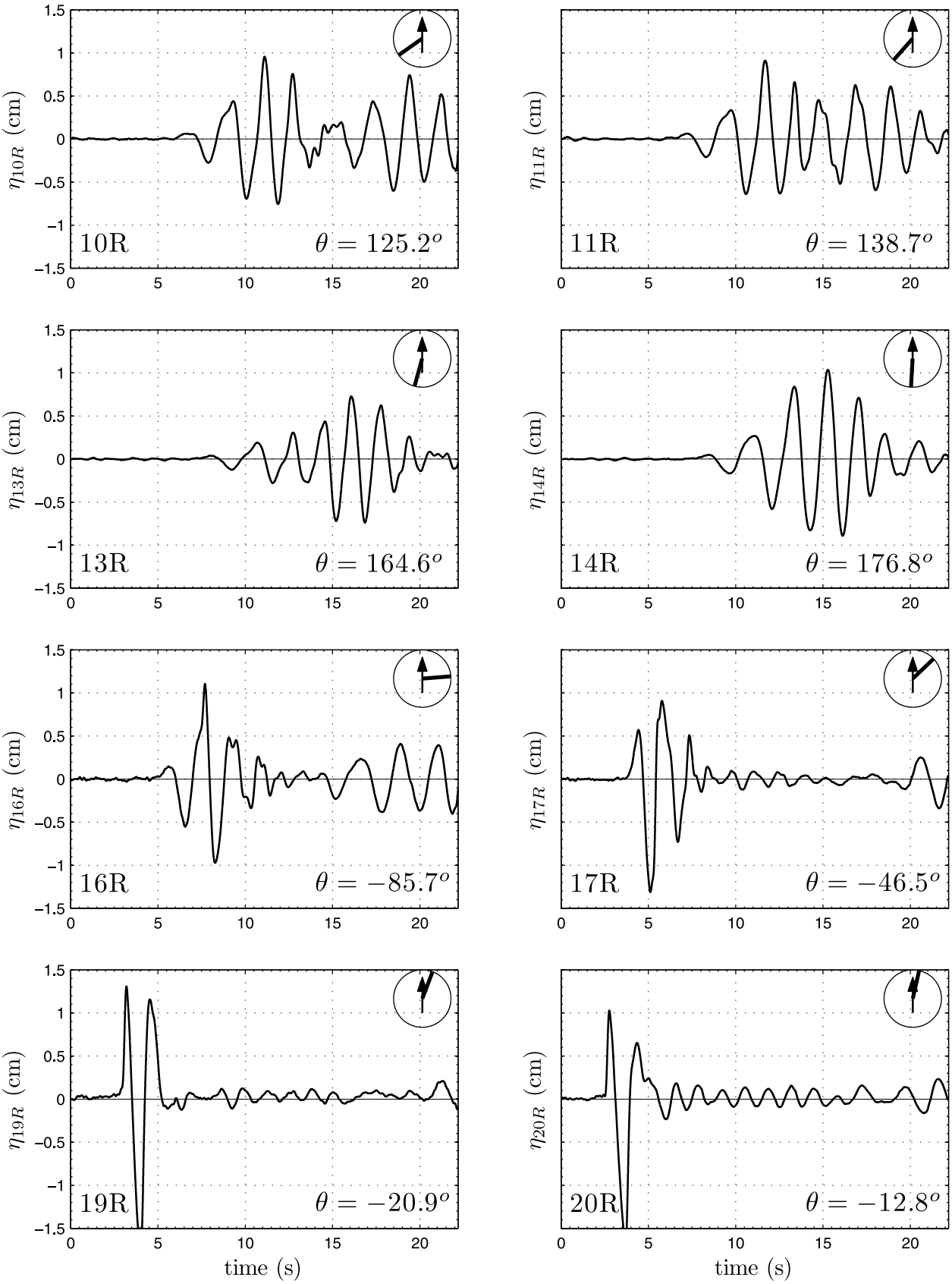

Figure 7. Notation. See Figure 6.

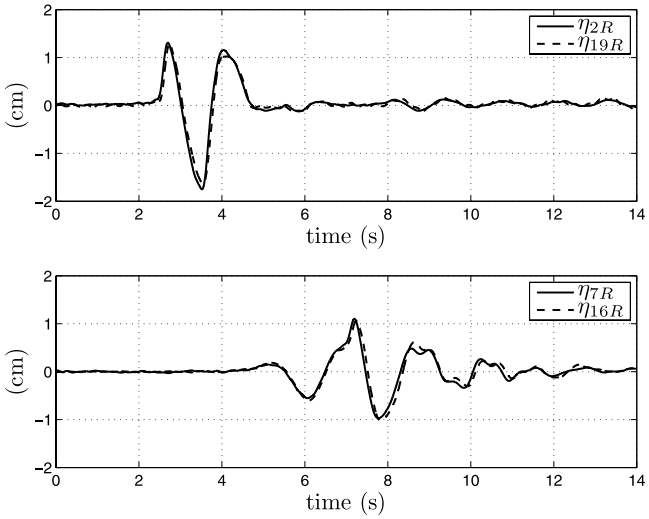

Figure 8. Comparison between time series measured at symmetrically placed runup gauges (2R and 19R in top and 7R and 16R in bottom) measured during experiment with ζ = 0.40 m and r_0 = 2.07 m.

pertaining to the third wave show again a very weak variation on ζ and appear highly repeatable, especially for higher values. The runup and the rundown, almost negligible in comparison to that induced by the other waves close to the generation area, gradually increase. $R_u^{(3)}$ appears to be always larger than $R_d^{(3)}$ (in absolute value). The results of the fourth wave are similar and again highly repeatable and weakly dependent on ζ.

[21] The effect of varying the radius of the undisturbed shoreline is shown in Figure 11 for the experiment carried out with ζ = 0.60 m. On each of the upper subplots the maximum runup and the minimum rundown for the three shoreline radius are presented by means of the same notation used before, but only data obtained for half of the island are shown. It is to be kept in mind that as the radius increases the distance between the runup gauges becomes larger, so the position of each gauge is given by a different value of s, which is the abscissa used in the plots. The first evidence is that as the radius r_0 increases also the runup increases. Furthermore, the position at which the maximum runup along the coast is measured moves away from the generation area for growing values of r_0. For r_0 = 2.07 m the $R_u^{(\max)}$ is at $s' \simeq 2$, for r_0 = 2.20 m at $s' \simeq 3.2$, for r_0 = 2.60 m at $s' \simeq 4$. In Figure 11 (bottom) we present the runup and the rundown induced by the first wave; the results of the two repetitions using ζ = 0.60 m are shown. The results are comparable to those obtained by Di Risio et al. (submitted manuscript, 2008), which, as said above, can be considered reliable, in the far field, only for the first part of the measurements (i.e., for the first wave only). Also for the first wave, runup increases when undisturbed shoreline radius (r_0) increases, and the point at which the maximum runup occurs moves away from the generation area. Results appear to be in agreement with those relative to the straight coast by Di Risio et al. (submitted manuscript, 2008), represented by the dark points, for which it is expected that the first wave runup reaches its maximum as the shoreline radius becomes infinite.

[22] In order to better describe the properties of the whole group of the first waves that propagate alongshore, the time series obtained at each runup gauge have been used to obtain the envelope of the instantaneous shoreline elevation. The elevation of the crests and of the troughs has therefore been used to estimate the parameters of the following function:

$$\eta_{env}(t) = a_{env}\mathrm{sech}[\Omega(t - t_0)] \tag{1}$$

where η_{env} is the time series of the wave envelope, a_{env} its amplitude, Ω is an angular frequency and t_0 the instant at which the maximum of the wave envelope occurs. Even if the wave envelope is not described by a periodic function, it is useful to define a wave envelope period (T_{env}) as follows:

$$T_{env}(\delta) = \frac{2\mathrm{sech}^{-1}(\delta/a_{env})}{\Omega} \tag{2}$$

that can be viewed as the time interval during which the wave envelope exceeds the threshold value δ. It has to be stressed that if one express the envelope period as $T_{env} = 2\pi/\Omega$, implicitly a threshold value δ for which $\delta/a_{env} \simeq 0.086$ is chosen. In the following we use a threshold value for which $\delta/a_{env} = 0.03$, in order to get an idea of the actual duration of the propagating wave group. On the basis of the experimental time series, for each runup gauge and for each test the parameters of the envelope (i.e., a_{env}, Ω and t_0) have been estimated by means of the Gauss-Newton non linear optimization method. Figure 12 shows the fitting results for the tests with undisturbed shoreline radius (r_0) equal to 2.20 m and for all the tested falling heights. It can be noted that the wave envelope is not affected by the landslide energy, that is, its falling height, as already found for the wave runup along the coast. The wave envelope amplitude decreases as the distance from the generation area grows and its period increases (Figure 13); this is the typical behavior of dispersive wave packets.

[23] The celerity of propagation around the coast of the island of both the crest and the trough of the first wave has been finally estimated. This has been calculated by evaluating the time that the crest and the trough take to propagate from one runup gauge to the next one; since the distance between the measurement points is known, an estimate of the celerity can be given. Results are presented in Figure 14 for all the experiments (two repetitions for each of the three shoreline radius and the four values of falling height ζ). The celerity is plotted against the distance s. It can be generally observed that the first wave tends to propagate faster as it moves away from the generation area. The celerity of the crest ($C_c^{(1)}$) appears to be larger than that of the trough ($C_t^{(1)}$), thus the wave lengthens as it propagates. The celerity estimated for the trough is less dispersed than that obtained using the crest.

5. Discussion

[24] The analysis of the runup gauges measurements raises several points of discussions. A point of interest is that the crest amplitude of the waves first increases with the distance from the generation area and then decreases. The crest of the first wave of the packet becomes very high close

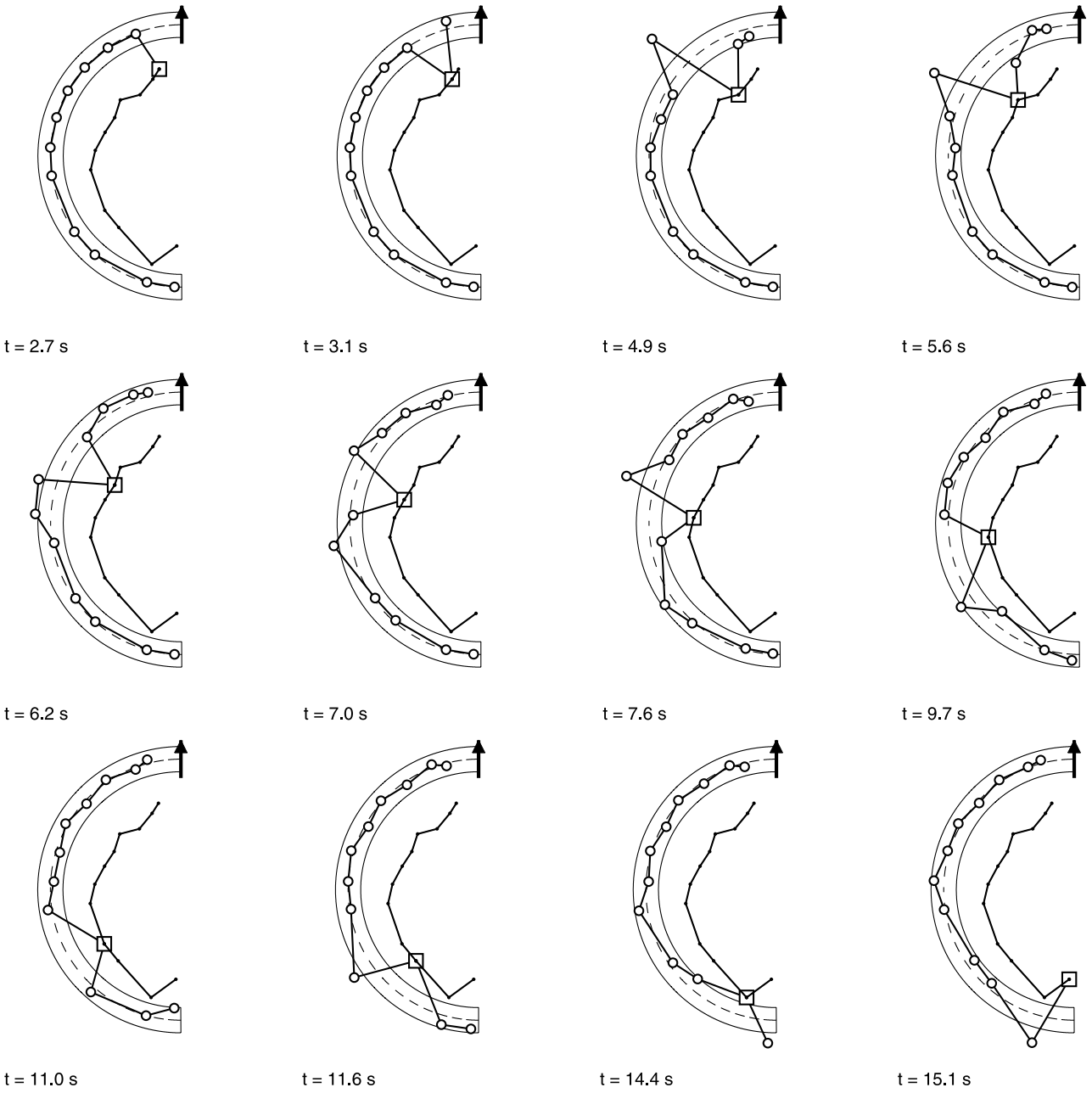

Figure 9. Snapshots of shoreline positions measured during experiment with $\zeta = 0.40$ m and $r_0 = 2.07$ m. The dashed semicircle is the undisturbed shoreline position, the thick solid line is the envelope of the runup, and the two solid semicircles give the scale and represent, respectively, a shoreline horizontal displacement equal to ±0.01 m.

to the landslide area in which it induces the maximum runup; then the second wave becomes more important, and for a certain distance it induces the largest inundation. Then the third wave grows and becomes the highest, and so on. This is the typical behavior of frequency dispersive waves, whose energy travels at the group celerity, which is smaller than that of the waves. Hence, even if in very shallow waters, the landslide generates a system of dispersive waves, similar to that of edge waves [*Ursell*, 1952] and has been observed in laboratory experiments [e.g., *Liu et al.*, 1998].

Figure 10. Observed values for (a) all the tested values of ζ and shoreline radius $R = 2.07$ m of maximum runup $R_u^{(\max)}$ and minimum rundown $R_d^{(\max)}$ (markers), (b) first wave runup $R_u^{(1)}$ and rundown $R_d^{(1)}$ (circles), (c) second wave runup $R_u^{(2)}$ and rundown $R_d^{(2)}$ (squares), (d) third wave runup $R_u^{(3)}$ and rundown $R_d^{(3)}$ (diamonds), and (e) fourth wave runup $R_u^{(4)}$ and rundown $R_d^{(4)}$ (triangles). Markers in Figure 10a indicate which wave has been observed to induce maximum runup and minimum rundown.

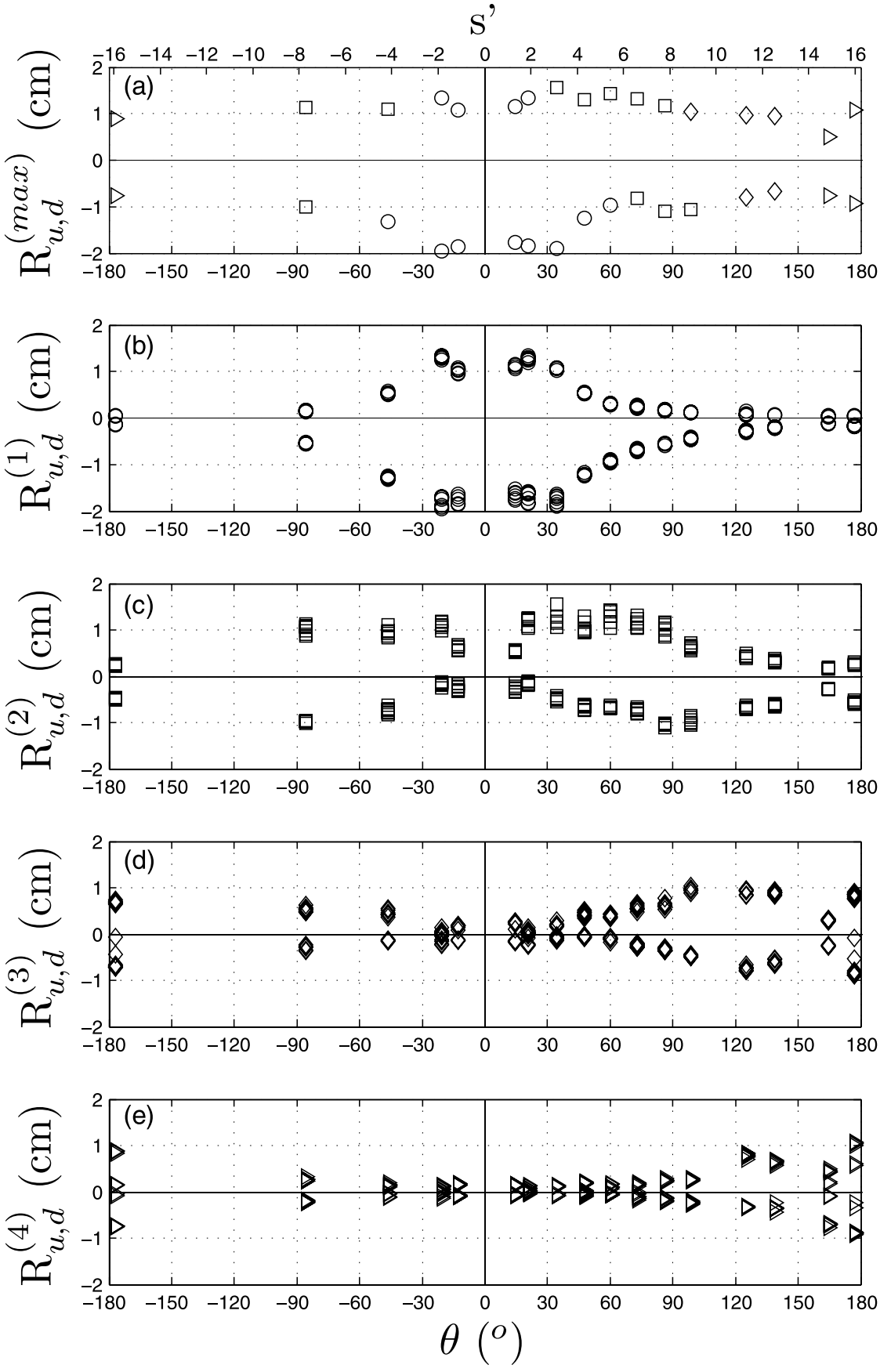

Figure 10

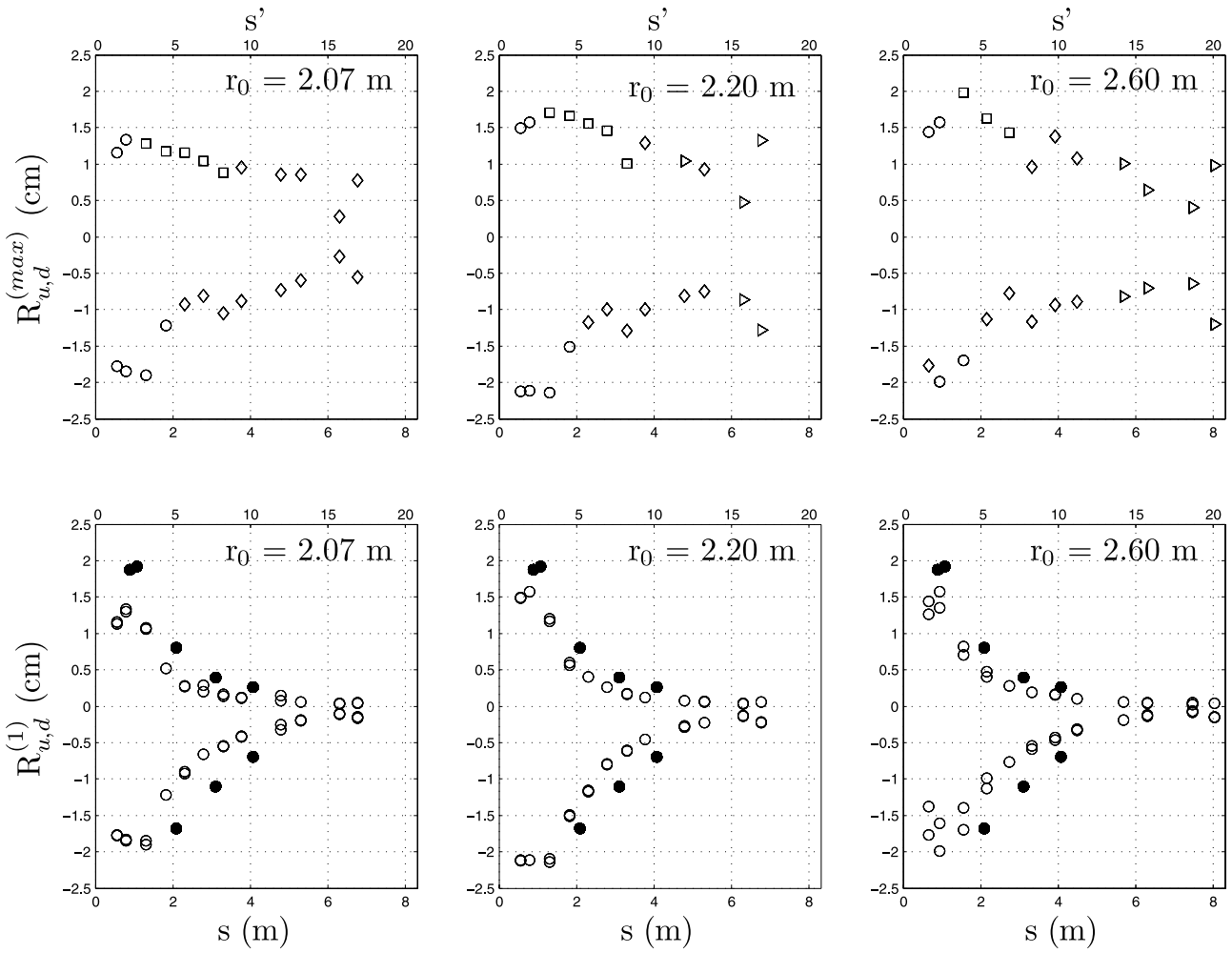

Figure 11. Observed values for z = 0.60 m and for all the tested shoreline radius of (top) maximum runup R_u and minimum rundown R_d and of the (bottom) first wave runup $R_u^{(1)}$ and rundown $R_d^{(1)}$. Solid circle in Figure 11 (top) indicates first wave runup and rundown reported by Di Risio et al. (submitted manuscript, 2008).

[25] A rough analysis of the contemporary results at the runup gauges allowed estimation of the order of magnitude of the waves' length. It has been found that their length is about 2.4 m (see Figure 9), that is, roughly equal to 6 times the width of the landslide. If we regard the model as a small-scale reproduction of a volcanic island, we can get an idea of what happened at the Stromboli island when a tsunamis was generated by a landslide in 2002 [*Tinti et al.*, 2005b]. By using the Froude similitude, and a scaling factor of λ = 1000 (note that the average radius of the island is of about 2 km and the average slope is 1:3), we can scale lengths as 1: λ, and times and velocities as 1: $\sqrt{\lambda}$; at prototype scale the length of the waves is then of about 2400 m. If a region along the coast is becoming inundated by the waves inducing the runup, at a half of the wavelength (i.e., at about 1200 m) from that point the water is receding, being the coast attacked by the trough of the waves. However experimental observations described above suggest that the crest of the first wave becomes very small at a distance of about 6 times the landslide width, if compared with the following trough and the subsequent waves' crest. People observing a receding shoreline are warned of the imminent attack of the crest of the following waves few seconds in advance: scaling up to prototype the average period of the waves in the laboratory (2 s) we conclude that after the first severe shoreline receding, the inundation will occur after about 30 s, that is, after a half of a wave period.

[26] It is important to stress that this discussion is entirely based on experimental observations of subaerial landslide effects. Usually, in the case of landslide generated tsunami, the source type may be inferred by observing if the wave-front is a crest, that is, a shoreline rising (subaerial land-

Figure 12. Wave envelopes for all the tested falling heights ζ and with shoreline radius r_0 equal to 2.20 m. Dashed lines represent runup time series, and solid lines represent the fitted wave envelope. The small circle on each plot reproduces the coastline, the arrow indicates where the landslide enters the water, and the line specifies the position of the considered runup gauge.

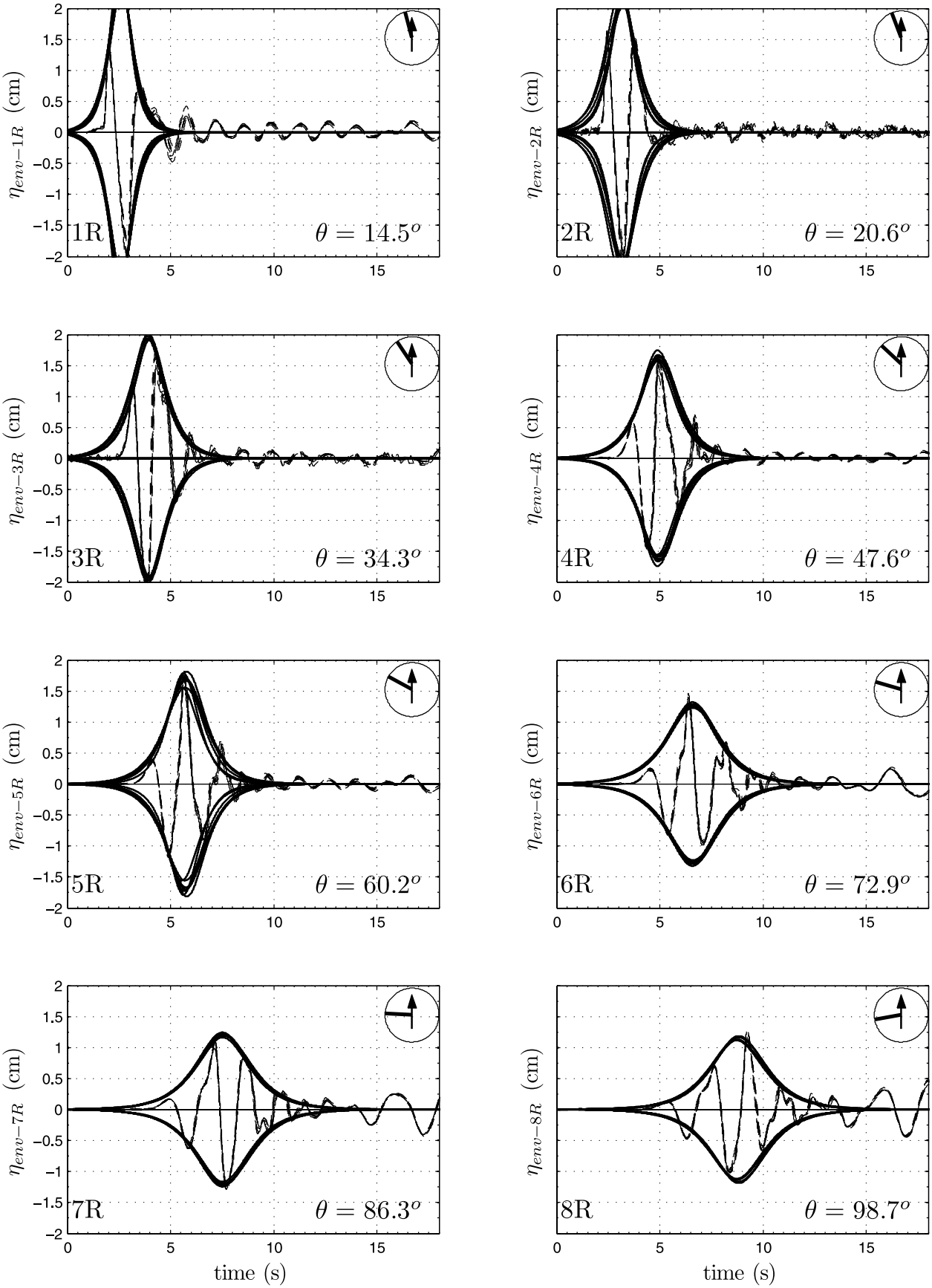
η_{env-1R} (cm)
1R
$\theta = 14.5^o$
η_{env-2R} (cm)
2R
$\theta = 20.6^o$
η_{env-3R} (cm)
3R
$\theta = 34.3^o$
η_{env-4R} (cm)
4R
$\theta = 47.6^o$
η_{env-5R} (cm)
5R
$\theta = 60.2^o$
η_{env-6R} (cm)
6R
$\theta = 72.9^o$
η_{env-7R} (cm)
7R
$\theta = 86.3^o$
η_{env-8R} (cm)
8R
$\theta = 98.7^o$
time (s)
time (s)

Figure 12

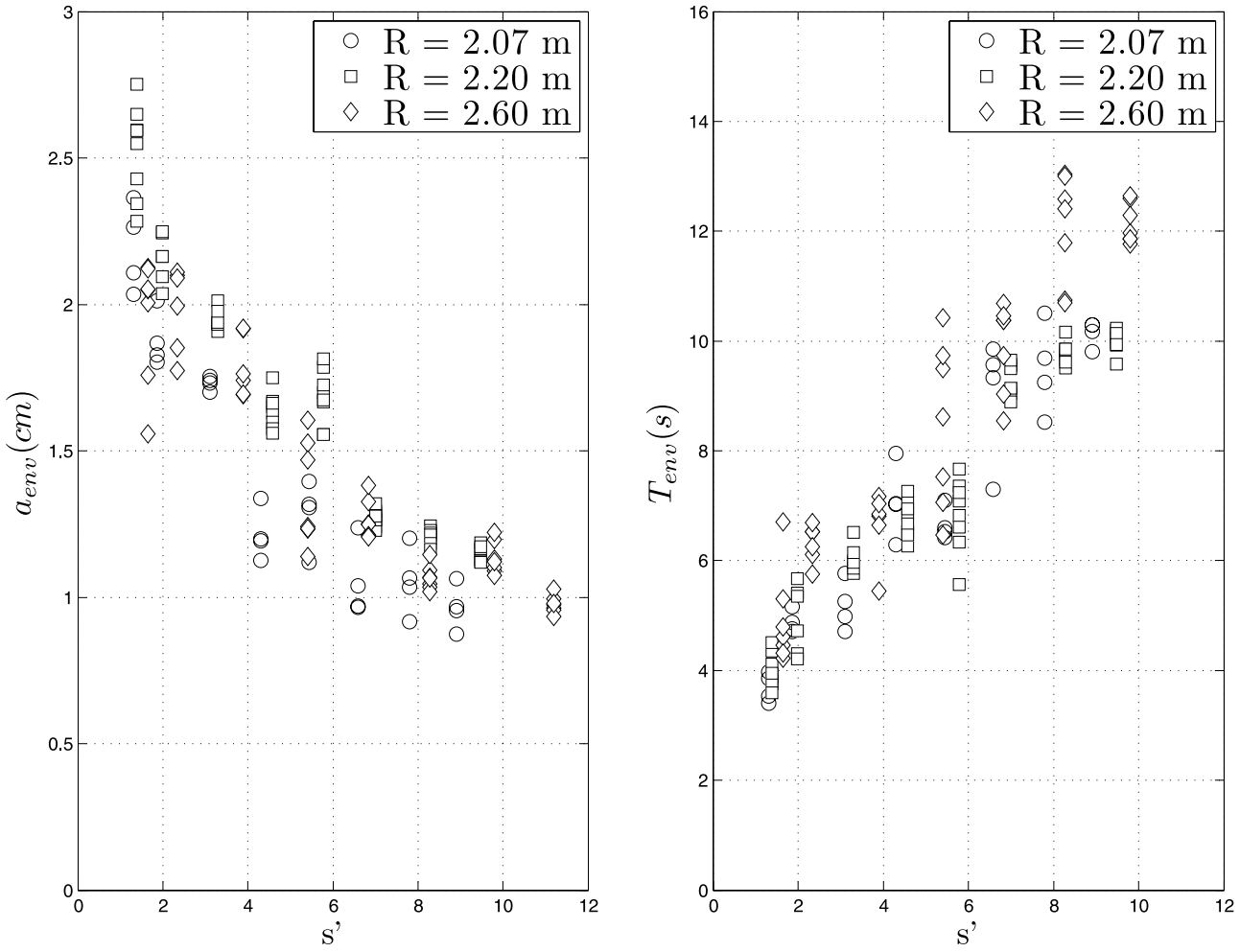

Figure 13. (left) Wave envelope amplitudes (a_{env}) and (right) period (T_{env}) variation against the dimensionless distance from generation area. Different markers refer to different shoreline radius (see legend).

slide), or a depression, that is, a shoreline receding (submerged landslide). However, also in the case of subaerial landslides the wavefront is a crest so small that at some distance from the source it is hardly detected: the first evidence of the tsunami attack is then the shoreline receding given by the trough of the first wave.

[27] The results, in terms of maximum runup and minimum rundown, have been found to depend very weakly on the falling height ζ. This result is consistent with that obtained using a similar layout by Di Risio et al. (submitted manuscript, 2008), and suggests that the wavefield is saturated, that is, the highest waves along the coast that the landslide model is able to generate have been reproduced. As far as the repeatability of the results is concerned we have found that some properties of the waves are highly repeatable (and are not influenced by ζ), others were, on the contrary, not satisfactorily repeatable neither using the same experimental conditions. A possible conclusion is that some wave properties are very stable (i.e., maximum runup and runup induced by the first wave), and quite insensitive to variations of landslide transfer of energy, at least for the range of the parameters investigated here. Other wave properties, such as the rundown induced in the near field by the trough of the first wave and, almost everywhere along the coast, the runup of the crest of the second wave appear to be very dependent also on very small changes of the parameters (i.e., landslide energy). This unexpected conclusion was already drawn, but not discussed in their paper, by Di Risio et al. (submitted manuscript, 2008). However in that work only the first wave was carefully measured, and the second one was contaminated by the reflected waves; the reason of the poor repeatability of this wave was therefore assigned to the reflected waves. It is worth to remember that the second wave is double peaked and that its crest is very sharp. We suspect that two or more wave components concur at determining its maximum elevation, and even very small shift of their phase can change the results. Of course this point deserves further theoretical investigation, and at the moment we limit to highlight it.

[28] The effect of varying the radius of the undisturbed shoreline has been investigated compatibly with the experimental facility, that is, without building further islands, but simply by varying the water depth. Decreasing the water depth has the effect that the radius of the coastline increases and that the path of the landslide under the water shortens.

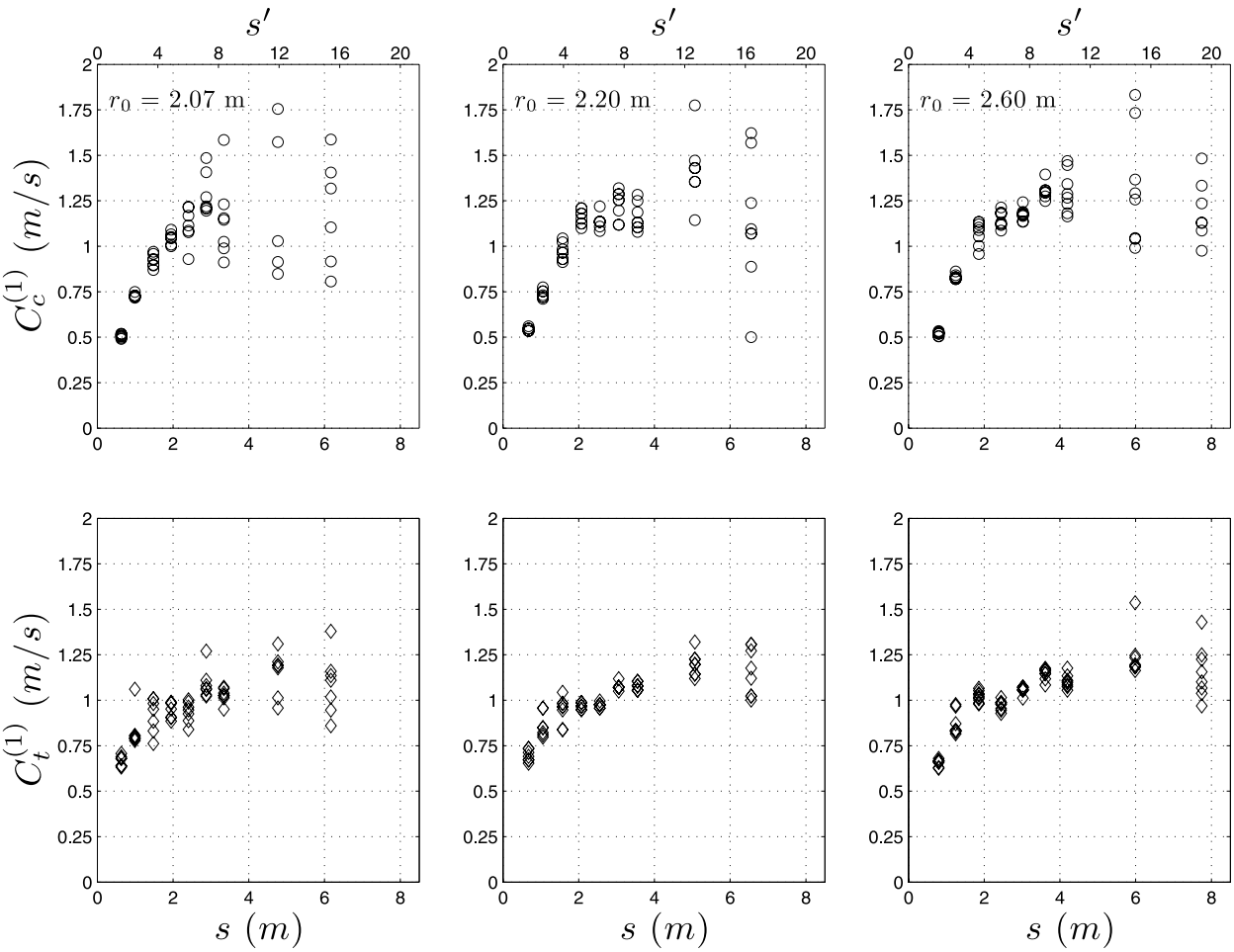

Figure 14. Wave celerity of the (top) first wave crest and (bottom) first wave trough for all the experiments.

On the one hand it is reasonable to expect the runup to increase as r_0 becomes larger, but on the other hand the landslide has a reduced ability of exchanging energy with the waves, since the time it interacts with the water is one of the crucial parameters that influence the energy exchange with the water [*Di Risio and Sammarco*, 2008]. The results however clearly indicate that the effect of the increasing radius of the shoreline is more important than that of the time of landslide-water interaction and the higher the undisturbed shoreline radius, the higher the induced runup.

6. Conclusions

[29] The experimental investigation described herein aimed at modeling landslide generated tsunamis occurring at the shoreline of a conical island. Despite the large body of work carried out to study the tsunami generation, propagation and interaction with coasts, very few three-dimensional researches focused on tsunami generated directly at the coast. This experimental research has considered a rigid landslide model constrained to slide down the flank of a conical island. The generated tsunami runup all around the island has been measured by means of special runup gauges. The results have allowed a detailed discussion of how the tsunami inundates the coast and what are the dominant properties of the waves. In the near field the wave runup grows, then at a distance larger than 2 times the landslide width it starts to decrease. The first wave is responsible of the maximum runup only in the near field and its crest becomes very small for $\theta > 90°$ where the third wave induces the maximum runup. The influence of the undisturbed shoreline radius has been observed to be important: the higher the radius, the higher the induced runup.

[30] **Acknowledgments.** This work was partially funded by the Italian Ministry of Research (MIUR) under the research projects "Development and validation of hydraulic and geologic tools for supporting a Tsunami Early Warning System. Implementation to the Stromboli landslide case" (PRIN-2004) and "Development and validation of hydraulic and geologic tools for supporting a Tsunami Early Warning System. Implementation to the Stromboli (Eolie) landslide case" (PRIN-2007). Thanks are due to the LIAM "Umberto Messina" technicians Mario Nardi and Lucio Matergia and to the LIC technicians Giuseppe Intranuovo and Luciano Romanazzi. Help of Luigi Pratola is acknowledged. We finally thank the two anonymous reviewers for their useful suggestions.

References

Briggs, M. J., C. E. Synolakis, G. S. Harkins, and D. R. Green (1995), Laboratory experiments on Tsunami runup on a conical island, *Pure Appl. Geophys.*, *144*(3/4), 569–593.

Di Risio, M., and P. Sammarco (2008), Analytical modeling of landslide generated waves, *J. Waterw. Port Coastal Ocean Eng.*, *134*(1), 1–69.

Enet, F., and S. T. Grilli (2005), Tsunami landslide generation: Modelling and experiments, paper presented at 5th Int. on Ocean Wave Measurement and Analysis WAVES 2005, IAHR, Madrid, Spain, 3-7 July.

Enet, F., and S. T. Grilli (2007), Experimental study of tsunami generation by three dimensional rigid underwater landslides, *J. Waterw. Port Coastal Ocean Eng.*, *133*(6), 442–454.

Enet, F., S. T. Grilli, and P. Watts (2003), Laboratory experiments for tsunamis generated by underwater landslides: Comparison with numerical modeling, in *Proc. of the 13th Offshore and Polar Eng. Conf.*, Honolulu, Hawaii, ISOPE03, vol. 3, pp. 372–379, ISOPE, Cupertino, Calif.

Fritz, H. M., W. H. Hager, and H.-E. Minor (2003a), Landslide generated impulse waves. 1: Instantaneous flow fields, *Exp. Fluids*, *35*(6), 505–519.

Fritz, H. M., W. H. Hager, and H.-E. Minor (2003b), Landslide generated impulse waves. 2: Hydrodynamic impact craters, *Exp. Fluids*, *35*(6), 520–532.

Grilli, S. T., and P. Watts (2005), Tsunami generation by submarine mass failure. I: Modeling, experimental validation, and sensitivity analyses, *J. Waterw. Port Coastal Ocean Eng.*, *131*(6), 283–297.

Heinrich, P. (1992), Nonlinear water waves generated by submarine and aerial landslides, *J. Waterw. Port Coastal Ocean Eng.*, *118*(3), 249–266.

Liu, P. L.-F., H. Yeh, P. Lin, K. T. Chang, and Y. S. Cho (1998), Generation and evolution of edge-wave packets, *Phys. Fluids*, *10*(7), 1635–1657.

Liu, P. L.-F., T.-R. Wu, F. Raichlen, C. E. Synolakis, and J. C. Borrero (2005), Runup and rundown generated by three-dimensional sliding masses, *J. Fluid Mech.*, *536*, 107–144.

Lynett, P., and P. L.-F. Liu (2005), A numerical study of the runup generated by three-dimensional landslides, *J. Geophys. Res.*, *110*, C03006, doi:10.1029/2004JC002443.

Panizzo, A., P. De Girolamo, and A. Petaccia (2005), Forecasting impulse waves generated by subaerial landslides, *J. Geophys. Res.*, *110*, C12025, doi:10.1029/2004JC002778.

Tinti, S., A. Maramai, A. Armigliato, L. Graziani, A. Manucci, G. Pagnoni, and F. Zaniboni (2005a), Observations of physical effects from tsunamis of December 30, 2002 at Stromboli volcano, southern Italy, *Bull. Volcanol.*, *68*(5), 450–461.

Tinti, S., A. Manucci, G. Pagnoni, A. Armigliato, and F. Zaniboni (2005b), The 30 December 2002 landslide-induced tsunamis in Stromboli: Sequence of the events reconstructed from the eyewitness accounts, *Nat. Hazards Earth Syst. Sci.*, *5*, 763–775.

Ursell, F. (1952), Edge waves on a sloping beach, *Proc. Royal Soc. London A*, *214*, 79–97.

Watts, P. (1997), Water waves generated by underwater landslides, Ph.D. dissertation, Calif. Inst. of Technol., Pasadena, Calif.

Watts, P. (1998), Wavemaker curves for tsunamis generated by underwater landslides, *J. Waterw. Port Coastal Ocean Eng.*, *124*(127).

Watts, P. (2000), Tsunami features of solid block underwater landslides, *J. Waterw. Port Coastal Ocean Eng.*, *126*(3), 144–152.

Wiegel, R. L. (1955), Laboratory studies of gravity waves generated by the movement of a submarine body, *Trans. AGU*, *36*(5), 759–774.

F. Aristodemo, Dipartimento di Difesa del Suolo, University of Calabria, Campus di Arcavacata, via P. Bucci, 87036 Arcavacata di Rende, Cosenza, Italy.

G. Bellotti, Dipartimento di Scienze dell'Ingegneria Civile, University of Roma Tre, Via Vito Volterra 62, 00146, Rome, Italy.

P. De Girolamo and M. Di Risio, Dipartimento di Ingegneria delle Strutture delle Acque e del Terreno, Laboratorio di Idraulica Ambientale e Marittima, University of L'Aquila, P.le Pontieri 1, Monteluco di Roio, 67040 L'Aquila, Italy. (mdirisio@ing.univaq.it)

M. G. Molfetta and A. F. Petrillo, Dipartimento di Ingegneria delle Acque e di Chimica, Laboratorio di Ricerca e Sperimentazione per la Difesa delle Coste, Technical University of Bari, S.P. Valenzano-Casamassima, Km. 3, 70010 Valenzano (Bari), Italy.

A. Panizzo, Dipartimento di Idraulica, Trasporti e Strade, University of Roma La Sapienza, via Eudossiana, 18, 00184 Rome, Italy.